Supplementary material

Supplementary methods

MRI examination protocol

Within a 7-day period after entry into the study, the MRI examination was performed using breath-holds by an experienced MRI technologist at the Department of Radiology, China-Japan Friendship Hospital, using a 3.0-T MR scanner (Ingenia; Philips Healthcare, Best, the Netherlands) with all subjects in a supine position. Subjects were restricted to nothing by mouth for 4 hours before imaging. An axial three-dimensional multi-echo modified Dixon gradient echo sequence (mDIXON-Quant), which has been described previously[1,2], was used for the hepatic steatosis assessment. The scan parameters for the mDIXON-Quant sequence were as follows: TR, 5.7 ms; TE1, 1.2 ms; 6 echoes with delta echo time (TE) 1.2 ms; field of view (FOV), 400× 350×210 mm; 3-mm slice thickness with no gap; flip angle (FA), 3°; voxel, 2.5 × 2.5 × 6.0 mm; matrix size = 200 × 222; number of slices = 70; scan time = 14s; SENSE = 2; number of signal average (NSA) =1. The mDIXON-Quant sequence automatically generates water, fat, fat-fraction, T_2*, and R_2* maps, along with in-phase and opposed-phase images that were synthesized from the water-fat images.

To estimate hepatic PDFF after image acquisition, circular region-of-interest (ROI) measurements of approximately 300 mm^2 in the liver were manually calculated in a fat-fraction map image, avoiding blood vessels, bile ducts, liver boundaries, focal hepatic lesions and artifacts (an example is shown in Supplementary Figure S2). Using a vendor-neutral postprocessing platform (Philips Interspace Portal, Philips Healthcare) for drawing ROIs on all fat-fraction maps, all subjects' fat-fraction maps were independently evaluated by a reviewer (SX) (with more than 10-years of experience of analyzing abdominal MRI) who was blinded to all clinical records. Three anatomically colocalized ROIs were placed in each of the nine Couinaud liver segments (namely, 27 separate ROIs in the whole liver) on the MR image

fat-fraction maps for each subject. The average from three colocalized ROIs measurements was documented as the representative hepatic PDFF for each hepatic segment, while the PDFF across the entire liver was defined as the average of 27 ROIs measurements for assessing hepatic steatosis. The liver fat-fraction map protocol and colocalization of ROIs were based on previous literature[3,4].

Supplementary Discussion

Rationale on MRI-PDFF as a surrogate gold standard of hepatic steatosis quantification

Firstly, MRI-PDFF has been proven to be an extremely precise, accurate and reproducible noninvasive biomarker for the quantitative determination of hepatic fat content[5]. Relevant research has indicated that MRI-PDFF correlates strongly with MRS (r^2=0.98, $P < 0.0001$)[3,6] and biopsy-proven steatosis grade (AUCs for the detection of steatosis grades ≥G1, ≥G2,and ≥G3, were 0.98, 0.91, and 0.92, respectively)[4,7-9]. Moreover, it performed better than ultrasound, computed tomography and even controlled attenuation parameter for the quantitative determination of hepatic fat content[10,11]. Secondly, since many patients with NAFLD need to receive regular follow-up regardless of the therapeutic intervention, frequent liver biopsy as an expensive and invasive operation is inappropriate and unethical. MRI-PDFF is also expensive; therefore, the use of noninvasive steatosis models capable of accurately diagnosing NAFLD as approximately MRI-PDFF ≥5% to screen subjects with NAFLD and non-NALFD may diminish much of the expenditure associated with follow-up monitoring. Furthermore, MRI-PDFF ≥5% as a diagnostic or inclusive standard for NAFLD has been widely applied in several previous studies and trials[12-15]. Thirdly, in order to assess and compare the accuracy of eight noninvasive steatosis biomarkers in diagnosing NAFLD, subjects without NAFLD were required, and it would be unethical to directly perform a liver biopsy in subjects without an appropriate clinical

indication for such a procedure[15].

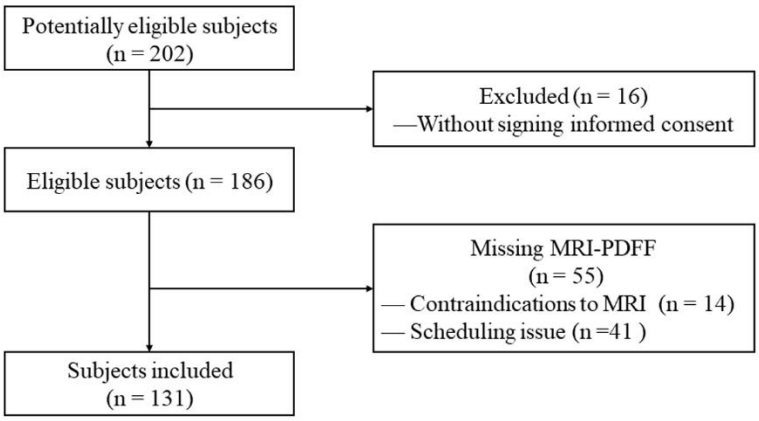

Supplementary Figure 1 Flow chart of the study population. Among 202 potentially eligible subjects, 16 did not provide written informed consent and 55 were excluded due to missing magnetic resonance imaging measurements. A total of 131 participants were ultimately included.

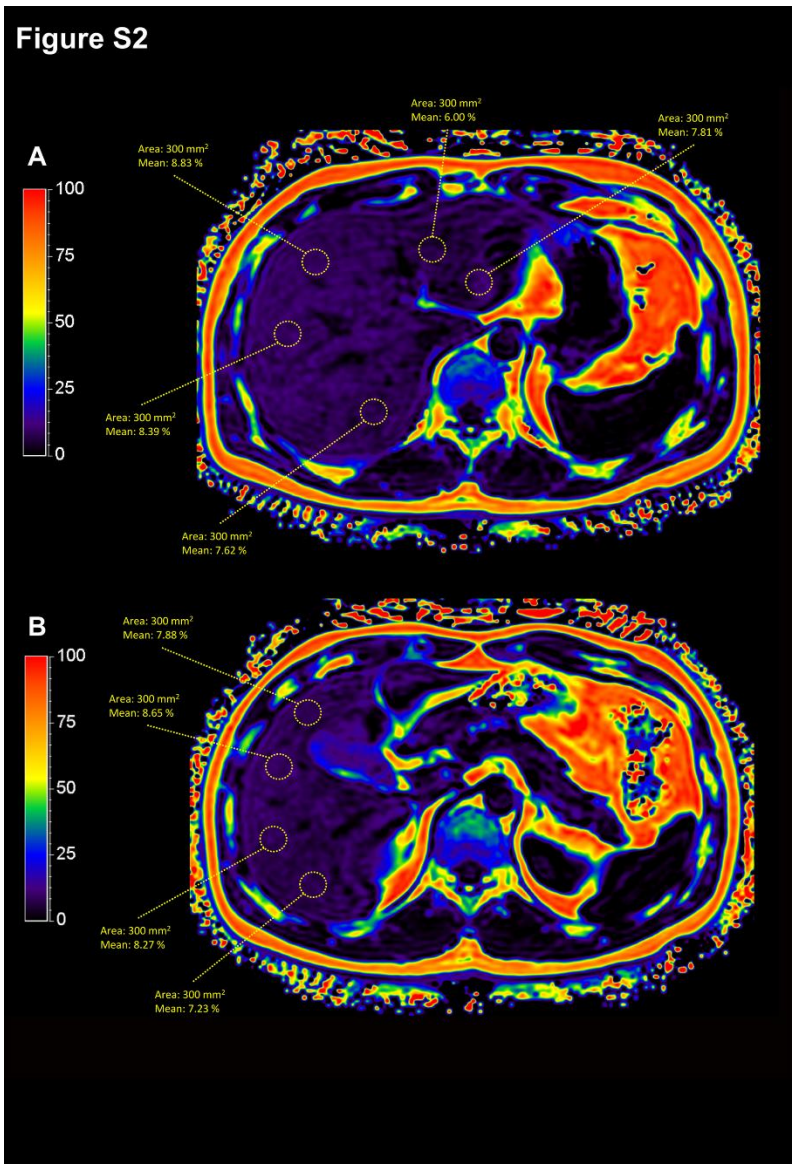

Supplementary Figure 2 Representative region-of interests drawn for calculating the proton density fat fraction value of the liver on magnetic resonance imaging fat-fraction maps (proton density fat fraction maps) generated automatically by the mDIXON-Quant sequence in a 27-year-old man with mildly elevated proton density fat fraction. A: Transverse sections through the left hepatic portal vein; B: Ttransverse sections through the splenic vein. All region-of-interests (ROIs) are distributed in the hepatic parenchyma, avoiding blood vessels, bile ducts, liver boundaries, focal hepatic lesions, and artifacts. The area of each ROI is approximately 300-400mm^2.

Supplementary Table 1 The percentage of participants identified by single optimal cut-offs, and the percentage of the presence and absence of nonalcoholic fatty liver disease per group

Biomarkers	Cut-off[1]	*n* (%) in category	*n* (%) with NAFLD	*n* (%) with non-NALFD
FLI (*n* = 131)				
	<42	44 (33.6)	15 (34.1)	29 (65.9)
	≥ 42	87 (66.4)	81 (93.1)	6 (6.9)
HSI (*n* = 131)				
	< 34	31 (23.7)	7 (22.6)	24 (77.4)
	≥ 34	100 (76.3)	89 (89.0)	11 (11.0)
ZJU index (*n* = 131)				
	< 37	34 (26.0)	8 (23.5)	26 (76.5)
	≥ 37	97 (74.0)	88 (90.7)	9 (9.3)
FSI (*n* = 131)				
	< 15	33 (25.2)	7 (21.2)	26 (78.8)
	≥ 15	98 (74.8)	89 (90.8)	9 (9.2)
TyG index (*n* = 131)				
	< 8.5	35 (26.7)	9 (25.7)	26 (74.3)
	≥ 8.5	96 (73.3)	87 (90.6)	9 (9.4)
VAI (*n* = 131)				
	< 1.49	40 (30.5)	12 (30.0)	28 (70.0)
	≥ 1.49	91 (69.5)	84 (92.3)	7 (7.7)

[1]The optimal cut-off with the highest Youden index.

FLI: Fatty liver index; HSI: Hepatic steatosis index; FSI: Framingham steatosis index; TyG: Triglycerides and glucose; VAI: Visceral adiposity index; NAFLD: Nonalcoholic fatty liver disease.

Supplementary Table 2 The percentage of participants identified by the previously established exclusionary and confirmatory cut-offs or single optimal cut-offs, and the percentage of the presence and absence of nonalcoholic fatty liver disease per group

Biomarkers	**Cut-off**	***n* (%) in category**	***n* (%) with NAFLD**	***n* (%) with non-NALFD**
Established dual cut-offs				
FLI (*n* = 131)				
Below exclusionary cut-off	<30	29 (22.1)	5 (17.2)	24 (82.8)
Intermediate	≥30 and <60	44 (33.6)	38 (86.4)	6 (13.6)
At or above confirmatory cut-off	≥60	58 (44.3)	53 (91.4)	5 (8.6)
HSI (*n* = 131)				
Below exclusionary cut-off	<30	11 (8.4)	0 (0.0)	11 (100)
Intermediate	≥30 and <36	27 (20.6)	13 (48.1)	14 (51.9)
At or above confirmatory cut-off	≥36	93 (71.0)	83 (89.2)	10 (10.8)
ZJU index (*n* = 131)				
Below exclusionary cut-off	<32	12 (9.2)	0 (0.0)	12 (100)
Intermediate	≥32 and <38	35 (26.7)	19 (54.3)	16 (45.7)
At or above confirmatory cut-off	≥38	84 (64.1)	77 (91.7)	7 (8.3)
Established single cut-offs				
FSI (*n* = 131)				
	<23	51 (38.9)	21 (41.2)	30 (58.8)
	≥23	80 (61.1)	75 (93.8)	5 (6.2)
TyG index (*n* = 131)				
	<8.5	35 (26.7)	9 (25.7)	26 (74.3)
	≥8.5	96 (73.3)	87 (90.6)	9 (9.4)

VAI (n = 131)				
	<1.25	32 (24.4)	7 (21.9)	25 (78.1)
	≥1.25	99 (75.6)	89 (89.9)	10 (10.1)

FLI: Fatty liver index; HSI: Hepatic steatosis index; FSI: Framingham steatosis index; TyG: Triglycerides and glucose; VAI: Visceral adiposity index; NAFLD: Nonalcoholic fatty liver disease.

Supplementary Table 3 The diagnostic accuracy of each noninvasive steatosis biomarker in excluding and confirming the presence of nonalcoholic fatty liver disease (magnetic resonance imaging proton density fat fraction ≥ 5%) by the established dual cut-offs or single optimal cut-offs

Biomarkers	AUC (95% CI)	SE, %	SP, %	PLR	NLR	PPV, %	NPV, %	Accuracy, %	Overall accuracy to exclude and confirm NAFLD, %
Established dual cut-offs									
FLI (*n* = 131)									
Exclusionary cut-off < 30	0.817 (0.740-0.879)	94.8	68.6	3.02	0.08	89.2	82.8	87.8	
Confirmatory cut-off ≥ 60	0.705 (0.619-0.781)	55.2	85.7	3.86	0.52	91.4	41.1	63.3	58.8
HSI (*n* = 131)									
Exclusionary cut-off < 30	0.657 (0.569-0.738)	100	31.4	1.46	0.00	80.0	100	81.7	
Confirmatory cut-off ≥ 36	0.789 (0.710-0.856)	86.5	71.4	3.03	0.19	89.2	65.8	82.4	71.8
ZJU index (*n* = 131)									
Exclusionary cut-off < 32	0.671 (0.584-0.751)	100.0	34.3	1.52	0.00	80.7	100	82.4	
Confirmatory cut-off ≥ 38	0.801 (0.722-0.866)	80.2	80.0	4.01	0.25	91.7	59.6	80.2	67.9

Established single cut-offs									
FSI (*n* = 131)									
Cut-off ≥ 23	0.819 (0.742-0.881)	78.1	85.7	5.47	0.26	93.7	58.8	80.2	n.a.
TyG index (*n* = 131)									
Cut-off ≥8.5	0.825 (0.748-0.885)	90.6	74.3	3.52	0.13	90.6	74.3	86.3	n.a.
VAI (*n* = 131)									
Cut-off ≥ 1.25	0.821 (0.744-0.882)	92.7	71.4	3.24	0.10	89.9	78.1	87.0	n.a.

AUC: Area under the receiver operating characteristic curve; 95%CI: 95% confidence interval; FLI: Fatty liver index; HSI: Hepatic steatosis index; FSI: Framingham steatosis index; TyG: Triglycerides and glucose; VAI: Visceral adiposity index; SE: Sensitivity; SP: Specificity; PLR: Positive likelihood ratio; NLR: Negative likelihood ratio; PPV: Positive predictive value; NPV: Negative predictive value; NAFLD: Nonalcoholic fatty liver disease; n.a.: Not applicable.

Supplementary Table 4 The percentage of participants identified by [1]exclusionary and confirmatory cut-offs in the present study, and the percentage of the presence and absence of nonalcoholic fatty liver disease per group[1]

Biomarkers	**Cut-off[2]**	***n* (%) in category**	***n* (%) with NAFLD**	***n* (%) with non-NALFD**
FLI (*n* = 131)				

Below exclusionary cut-off	<20	20 (15.3)	1 (5.0)	19 (95.0)
Intermediate	≥20 and <68	65 (49.6)	51 (78.5)	14 (21.5)
At or above confirmatory cut-off	≥68	46 (35.1)	44 (95.7)	2 (4.3)
HSI (*n* = 131)				
Below exclusionary cut-off	<33	21(16.0)	1 (4.8)	20 (95.2)
Intermediate	≥33 and <39	43 (32.8)	31 (72.1)	12 (27.9)
At or above confirmatory cut-off	≥39	67 (51.1)	64 (95.5)	3 (4.5)
ZJU index (*n* = 131)				
Below exclusionary cut-off	<34	20 (15.3)	1 (5.0)	19 (95.0)
Intermediate	≥34 and <41	59 (45.0)	45 (76.3)	14 (23.7)
At or above confirmatory cut-off	≥41	52 (39.7)	50 (96.2)	2 (3.8)
FSI (*n* = 131)				
Below exclusionary cut-off	<7	22 (16.8)	2 (9.1)	20 (90.9)
Intermediate	≥7 and <42	61 (46.6)	48 (78.7)	13 (21.3)
At or above confirmatory cut-off	≥42	48 (36.6)	46 (95.8)	2 (4.2)
TyG index (*n* = 131)				
Below exclusionary cut-off	<8.0	14 (10.7)	0 (0.0)	14 (100)

Intermediate	≥8.0 and <9.2	78 (59.5)	59 (75.6)	19 (24.4)
At or above confirmatory cut-off	≥9.2	39 (29.8)	37 (94.9)	2 (5.1)
VAI (*n* = 131)				
Below exclusionary cut-off	<0.79	11 (8.4)	1 (9.1)	10 (90.9)
Intermediate	≥0.79 and <3.29	90 (68.7)	67 (74.4)	23 (25.6)
At or above confirmatory cut-off	≥3.29	30 (22.9)	28 (93.3)	2 (6.7)

[1]Criteria for the confirmatory cut-off were specificity >90% and positive likelihood ratio ≥ 10.

[2]Criteria for the exclusionary cut-off were sensitivity >90% and negative likelihood ratio ≤ 0.1.

FLI: Fatty liver index; HSI: Hepatic steatosis index; FSI: Framingham steatosis index; TyG: Triglycerides and glucose; VAI: Visceral adiposity index; NAFLD: Nonalcoholic fatty liver disease.

Supplementary Table 5 The diagnostic performance of each steatosis biomarker for predicting moderate-to-severe steatosis (magnetic resonance imaging proton density fat fraction ≥ 11%) or severe steatosis (magnetic resonance imaging proton density fat fraction ≥ 17%)

Biomarkers	AUC (95%CI)	Cut-off[1]	SE, %	SP, %	PLR	NLR	PPV, %	NPV, %	Accuracy, %
Moderate-to-severe steatosis									

FLI	0.818 (0.741-0.880)	≥58	81.3	74.7	3.21	0.25	65.0	87.3	75.6
HSI	0.857 (0.785-0.912)	≥39	89.6	71.1	3.10	0.15	64.2	92.2	77.1
ZJU index	0.854 (0.781-0.909)	≥39	95.8	67.5	2.95	0.06	63.0	96.6	76.3
FSI	0.852 (0.779-0.908)	≥35	85.4	77.1	3.73	0.19	68.3	90.1	68.7
TyG index	0.732 (0.648-0.806)	≥8.8	81.3	59.0	1.98	0.32	53.4	84.5	65.6
VAI	0.704 (0.618-0.831)	≥1.51	91.7	44.6	1.65	0.19	48.9	90.2	61.1
Severe steatosis									
FLI	0.829 (0.754-0.889)	≥58	91.3	63.9	2.53	0.14	35.0	97.2	67.2
HSI	0.852 (0.779-0.908)	≥41	82.6	76.9	3.57	0.23	43.2	95.4	71.0
ZJU index	0.851 (0.779-0.908)	≥41	87.0	74.1	3.35	0.18	41.7	96.4	73.3
FSI	0.832 (0.757-0.892)	≥45	82.6	78.7	3.88	0.22	45.2	95.5	59.5
TyG index	0.730 (0.646-0.804)	≥8.8	91.3	51.9	1.90	0.17	28.8	96.6	57.3
VAI	0.711 (0.626-0.787)	≥2.28	73.9	63.9	2.05	0.41	30.4	92.0	64.1

[1]The optimal cut-off with the highest Youden index.

AUC: Area under the receiver operating characteristic curve; 95%CI: 95% confidence interval; FLI: Fatty liver index; HSI: Hepatic steatosis index; FSI: Framingham steatosis index; TyG: Triglycerides and glucose; VAI: Visceral adiposity index; SE: Sensitivity; SP:

Specificity; PLR: Positive likelihood ratio; NLR: Negative likelihood ratio; PPV: Positive predictive value; NPV: Negative predictive value.

References

1 **Zhang Y**, Wang C, Duanmu Y, Zhang C, Zhao W, Wang L, Cheng X, Veronese N, Guglielmi G. Comparison of CT and magnetic resonance mDIXON-Quant sequence in the diagnosis of mild hepatic steatosis. *Br J Radiol* 2018; **91**: 20170587 [PMID: 30028193 DOI: 10.1259/bjr.20170587]

2 **Bhat V**, Velandai S, Belliappa V, Illayraja J, Halli KG, Gopalakrishnan G. Quantification of Liver Fat with mDIXON Magnetic Resonance Imaging, Comparison with the Computed Tomography and the Biopsy. *J Clin Diagn Res* 2017; **11**: TC06-TC10 [PMID: 28892997 DOI: 10.7860/JCDR/2017/26317.10234]

3 **Noureddin M**, Lam J, Peterson MR, Middleton M, Hamilton G, Le TA, Bettencourt R, Changchien C, Brenner DA, Sirlin C, Loomba R. Utility of magnetic resonance imaging versus histology for quantifying changes in liver fat in nonalcoholic fatty liver disease trials. *Hepatology* 2013; **58**: 1930-1940 [PMID: 23696515 DOI: 10.1002/hep.26455]

4 **Tang A**, Desai A, Hamilton G, Wolfson T, Gamst A, Lam J, Clark L, Hooker J, Chavez T, Ang BD, Middleton MS, Peterson M, Loomba R, Sirlin CB. Accuracy of MR imaging-estimated proton density fat fraction for classification of dichotomized histologic steatosis grades in nonalcoholic fatty liver disease. *Radiology* 2015; **274**: 416-425 [PMID: 25247408 DOI: 10.1148/radiol.14140754]

5 **Wong VW**, Adams LA, de Lédinghen V, Wong GL, Sookoian S. Noninvasive biomarkers in NAFLD and NASH - current progress and future promise. *Nat Rev Gastroenterol Hepatol* 2018; **15**: 461-478 [PMID: 29844588 DOI: 10.1038/s41575-018-0014-9]

6 **Zheng D**, Guo Z, Schroder PM, Zheng Z, Lu Y, Gu J, He X. Accuracy of MR Imaging and MR Spectroscopy for Detection and Quantification of Hepatic

Steatosis in Living Liver Donors: A Meta-Analysis. *Radiology* 2017; **282**: 92-102 [PMID: 27479639 DOI: 10.1148/radiol.2016152571]

7 **Imajo K**, Kessoku T, Honda Y, Tomeno W, Ogawa Y, Mawatari H, Fujita K, Yoneda M, Taguri M, Hyogo H, Sumida Y, Ono M, Eguchi Y, Inoue T, Yamanaka T, Wada K, Saito S, Nakajima A. Magnetic Resonance Imaging More Accurately Classifies Steatosis and Fibrosis in Patients With Nonalcoholic Fatty Liver Disease Than Transient Elastography. *Gastroenterology* 2016; **150**: 626-637.e7 [PMID: 26677985 DOI: 10.1053/j.gastro.2015.11.048]

8 **Middleton MS**, Heba ER, Hooker CA, Bashir MR, Fowler KJ, Sandrasegaran K, Brunt EM, Kleiner DE, Doo E, Van Natta ML, Lavine JE, Neuschwander-Tetri BA, Sanyal A, Loomba R, Sirlin CB; NASH Clinical Research Network. Agreement Between Magnetic Resonance Imaging Proton Density Fat Fraction Measurements and Pathologist-Assigned Steatosis Grades of Liver Biopsies From Adults With Nonalcoholic Steatohepatitis. *Gastroenterology* 2017; **153**: 753-761 [PMID: 28624576 DOI: 10.1053/j.gastro.2017.06.005]

9 **Qu Y**, Li M, Hamilton G, Zhang YN, Song B. Diagnostic accuracy of hepatic proton density fat fraction measured by magnetic resonance imaging for the evaluation of liver steatosis with histology as reference standard: a meta-analysis. *Eur Radiol* 2019; **29**: 5180-5189 [PMID: 30877459 DOI: 10.1007/s00330-019-06071-5]

10 **Bohte AE**, van Werven JR, Bipat S, Stoker J. The diagnostic accuracy of US, CT, MRI and 1H-MRS for the evaluation of hepatic steatosis compared with liver biopsy: a meta-analysis. *Eur Radiol* 2011; **21**: 87-97 [PMID: 20680289 DOI: 10.1007/s00330-010-1905-5]

11 **Dulai PS**, Sirlin CB, Loomba R. MRI and MRE for non-invasive

quantitative assessment of hepatic steatosis and fibrosis in NAFLD and NASH: Clinical trials to clinical practice. *J Hepatol* 2016; **65**: 1006-1016 [PMID: 27312947 DOI: 10.1016/j.jhep.2016.06.005]

12 **Le TA**, Chen J, Changchien C, Peterson MR, Kono Y, Patton H, Cohen BL, Brenner D, Sirlin C, Loomba R; San Diego Integrated NAFLD Research Consortium (SINC). Effect of colesevelam on liver fat quantified by magnetic resonance in nonalcoholic steatohepatitis: a randomized controlled trial. *Hepatology* 2012; **56**: 922-932 [PMID: 22431131 DOI: 10.1002/hep.25731]

13 **Loomba R**, Sirlin CB, Ang B, Bettencourt R, Jain R, Salotti J, Soaft L, Hooker J, Kono Y, Bhatt A, Hernandez L, Nguyen P, Noureddin M, Haufe W, Hooker C, Yin M, Ehman R, Lin GY, Valasek MA, Brenner DA, Richards L; San Diego Integrated NAFLD Research Consortium (SINC). Ezetimibe for the treatment of nonalcoholic steatohepatitis: assessment by novel magnetic resonance imaging and magnetic resonance elastography in a randomized trial (MOZART trial). *Hepatology* 2015; **61**: 1239-1250 [PMID: 25482832 DOI: 10.1002/hep.27647]

14 **Cui J**, Philo L, Nguyen P, Hofflich H, Hernandez C, Bettencourt R, Richards L, Salotti J, Bhatt A, Hooker J, Haufe W, Hooker C, Brenner DA, Sirlin CB, Loomba R. Sitagliptin vs. placebo for non-alcoholic fatty liver disease: A randomized controlled trial. *J Hepatol* 2016; **65**: 369-376 [PMID: 27151177 DOI: 10.1016/j.jhep.2016.04.021]

15 **Caussy C**, Alquiraish MH, Nguyen P, Hernandez C, Cepin S, Fortney LE, Ajmera V, Bettencourt R, Collier S, Hooker J, Sy E, Rizo E, Richards L, Sirlin CB, Loomba R. Optimal threshold of controlled attenuation parameter with MRI-PDFF as the gold standard for the detection of hepatic steatosis. *Hepatology* 2018; **67**: 1348-1359 [PMID: 29108123 DOI: 10.1002/hep.29639]